Application of the Schmidt hammer in the relative-age dating of rockfall deposits in the Belvedere Glacier Valley

Jan Baťka[1,*], Roberto Sergio Azzoni[2], Vít Vilímek[1]

[1] Charles University, Faculty of Science, Department of Physical Geography and Geoecology, Czechia
[2] University of Milan, Earth Science Department, "A. Desio", Italy
* Corresponding author: jan.batka@natur.cuni.cz

ABSTRACT

The Schmidt hammer is a cost-effective tool for both relative- and absolute-age dating of rocks (the latter in connection with previously absolutely dated surfaces). Its application in high-mountain environments is particularly favoured due to the abundance of dating material and the small size of the dating tool compared to other options. The use of the Schmidt hammer on rock types with macroscopic crystals is not recommended due to the varying weathering rates of different minerals. However, in harsh alpine conditions, there is often no other choice. We applied the Schmidt hammer in the relative dating of boulders in the Belvedere Glacier valley (Italian Alps) with orthogneiss and paragneiss being the dominant rock types (both consisting of macroscopic minerals). For the first time in the Schmidt hammer-related studies, we prepared a chart for the objective inclination correction of the data. The correction for aspect was also performed. The results suggest the successful applicability of the Schmidt hammer even under the unfavourable circumstances.

KEYWORDS

Schmidt hammer; relative dating; rockfalls; weathering; Belvedere Glacier

Received: 19 April 2024
Accepted: 28 November 2024
Published online: 16 December 2024

Baťka, J., Azzoni, R. S., Vilímek, V. (2024): Application of the Schmidt hammer in the relative-age dating of rockfall deposits in the Belvedere Glacier Valley. AUC Geographica 59(2), 272–281
https://doi.org/10.14712/23361980.2024.25

1. Introduction

The Schmidt hammer was originally developed for non-destructive testing of the strength of concrete by the Swiss engineer, Ernst Schmidt, whose goal was to measure the deterioration rate of concrete structures over time (Schmidt 1950). It consists of a spring-loaded piston and a plunger, which is pressed against the surface. Thereby, the piston is released and its impact onto the plunger transfers the energy to the material (Aydin 2015). A certain part of the energy is transformed into heat, sound, and surface deformation, the rest is recovered forcing the piston to rebound (Goudie 2006). The amount of recovered energy depends on the hardness of the material and is measured as a percentage of the maximum stretch length of the spring before release, the so-called R value (Aydin 2015).

The potential of this new instrument for environmental science was first exploited by Yaalon and Singer (1974) and Day and Goudie (1977) in the assessment of rock hardness. Matthews and Shakesby (1984) and Betts and Latta (2000) conducted pivotal studies of the use of the Schmidt hammer in relative- and numerical-age dating, respectively. The new technique steadily gained attention and found its application in the dating of various geomorphological events and landforms (fully summarised by Matthews and Winkler 2022): bedrock and moraine ridges formed during the Late Pleistocene deglaciation and Younger Dryas (Longhi et al. 2024; Longhi and Guglielmin 2020; Tomkins et al. 2018, 2016; Engel et al. 2011), paraglacial rockfalls and alluvial fans (McEwen et al. 2020; Scotti et al. 2017), rock glaciers and other periglacial landforms (Marr et al. 2022; Nesje et al. 2021), coastal landscapes (Sjöberg and Broadbent 1991), fluvial terraces (Stahl et al. 2013), and slope movements in tropical and temperate environments (Burda et al. 2018; Klimeš et al. 2009). The strong supremacy of glacial or permafrost environment-related research has an obvious reason, i.e., the abundance of dating material.

Contrary to the above, the studies of the weathering itself that use the Schmidt hammer show larger diversity, as reviewed by Goudie (2006). The possible applications include karstic forms (Haryono and Day 2004), tafoni and shore platforms (Stephenson and Kirk 2000; Matsukura and Matsuoka 1996), development of inselbergs (Pye et al. 1986), weathering-based rock classification (Karpuz and Paşamehmetoğlu 1997), temporal changes of weathering rates (White et al. 1998; Sjöberg and Broadbent 1991), and the relation between aspect and weathering rates (Waragai 1999).

Application of the Schmidt hammer for numerical-age dating requires a set of pre-dated control points for the calculation of calibration curves between the R value and absolute age. Commonly, a few control points are dated using terrestrial cosmogenic nuclide dating. The bulk of the surface exposure-ages are then determined with calibrated R values as the high cost of the nuclide technique prevents its more extensive application (Matthews and Winkler 2022). When only relative ages are needed, the considerably cheaper Schmidt hammer proves to be a robust dating tool (Shakesby 2006). The constraints of the technique include its sensitiveness to moisture content, and influence of surface texture, as well as rock inhomogeneity, on the results (Goudie 2006). However, the study of high mountain environments often offers only macroscopically inhomogeneous rocks, such as orthogneiss. Should they be a priori precluded from Schmidt hammer studies or is there any potential for reliable relative data?

Our aim was to apply the Schmidt hammer for relative age dating of orthogneiss and paragneiss boulders in the Belvedere Glacier valley (the Italian Alps). The inspected blocks of complex glacial and periglacial origin span temporally from rather fresh supraglacial samples to more weathered ones partly buried in the flat sedimentary plain neighbouring the glacier. We created a systematic chart for the inclination corrections, the first one ever published and based on the findings by Basu and Aydin (2004). Lastly, we examine the plausibility of the results and discuss them in a broader geomorphological context.

2. Study area

The Belvedere Glacier is a valley glacier located at the foot of the northeastern (i.e., Italian) face of the well-known Monte Rosa (4634 m a.s.l.). It is fed by frequent snow and ice avalanches from the surrounding steep hanging glaciers. The altitudinal range of the debris-covered tongue reaches approximately 400 m stretching from about 1800 to 2200 m a.s.l. (Fig. 1). The glacier occupies the orographic left (western) part of a broader valley carved during the Pleistocene glaciations with its left lateral moraine partially leaning against a valley side. The right lateral moraine neighbours a moraine-dammed lake named Lago delle Locce in the uppermost section, oversights an almost flat plain littered with boulders in the central part (Fig. 5), and in the lower section steeply descends into a gorge of the stream that drains the eastern portion of the catchment. The valley runs in a north-south direction and turns to the northeast near the head of the gorge. It takes another 45° turn towards the east some 650 metres downstream, at the point where the Belvedere Glaciers splits into two lobes. Both lobes terminate well above the mountainous village of Macugnaga.

The valley is significantly shaped by snow and ice avalanches that feed the glacier and often deposit fresh rock debris on its surface. Fresh taluses on the valley sides suggest the activity of rockfalls related to the structural changes of steep rock faces caused by thawing permafrost. Moraine lobes accumulated during

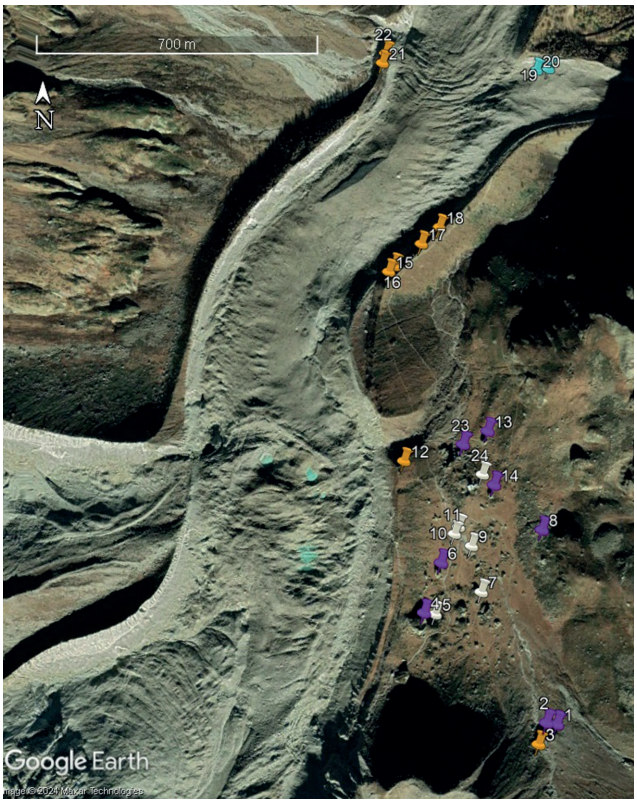

Fig. 1 Location of the sampled boulders within the Belvedere Glacier valley; boulders on the surface in violet; partly buried boulders in white; boulders in moraine in orange; supraglacial boulders in blue.

the Little Ice Age witnessed steady glacier retreat during the last century with the occasional formation of several moraine-dammed lakes. The largest one, the Lago delle Locce, was the source of a significant glacial flood event in 1978, and therefore was an object of remedial works in the 1980s (Haeberli and Epifani 1986). The Belvedere Glacier experienced an unexpected surge event in 2001–2003 (Kääb et al. 2004), whereafter it underwent a continuous downwasting. The glacial flood and surge events formed several overspills of the right lateral moraine and a significant V-shaped breach with outwash accumulations at the head of the gorge. The debuttressing of the moraine slopes caused by the lowering of the Belvedere Glacier surface is demonstrated by numerous small slides and the fresh surface of the inner moraine slopes.

The geology of the Monte Rosa east face is characterized by layers of two different lithologies: orthogneiss and paragneiss. The two lithologies stem from the crystalline of the Penninic Monte Rosa nappe. The composition of orthogneiss varies considerably throughout the Monte Rosa east face but the predominant constituent minerals are always quartz, K-feldspar, plagioclase, muscovite and biotite. Paragneiss contains either biotite or muscovite as a main part, often combined as well, and garnet, quartz and feldspar as a minor part. The paragneiss shows a pronounced parallel texture (schistosity) with varying formation from schist to gneiss (Fisher et al. 2006).

3. Methods

3.1 Data collection

The readings were gathered during three cloudy but dry days in August 2022 (9th–11th) and 2023 (1st–2nd). A standard Proceq N-type Schmidt hammer (Proceq SA N-34) was operated by three alternating researchers generally following standard recommendations (e.g., Aydin 2015; Day and Goudie 1977). Each measurement was made perpendicular to the surface while avoiding sharp edges, cracks, fissures, weathering rinds, and visibly exfoliating slabs. In several cases, exfoliating flakes hidden under the boulder surface were indicated after impact by a typical sound resembling a machine gun. The locations with the least microtopography were selected, the task being hindered by the heterogeneous nature of the orthogneiss. Preferably, the surfaces covered in lichens were avoided despite the difficulty of the task as these thrive in the cold humid climate of the Belvedere Glacier valley.

The mineralogical structure of the boulder surface was largely obscured by the severe effects of weathering. Therefore, a bias may have arisen from repeated measurements of harder (or softer) minerals of the heterogeneous orthogneiss. To compensate for this, three measurements, all of which were taken from locations typically a few centimetres apart from each other, were averaged. This means that each reading is an average rock hardness value of a small area on the boulder's surface. The neighbouring readings were usually distanced at least 10 centimetres. The record of each reading contains the boulder-related information (location, position, rock type, size) and the aspect and inclination of the small area from which it was taken (Tab. 1).

3.2 Correction for the impact angle

As the Schmidt hammer measures the rebound of the piston after the impact, gravity may facilitate (impact on overhanging surfaces) or hinder (impact on sloping or flat surfaces) the rebound. The largest and zero effect of gravity is recorded after impacts in the vertical and horizontal direction, respectively. The original correction chart for the impact angle was designed by the manufacturer for measurements of concrete hardness and was corrected by Basu and Aydin (2004) for field rock hardness measurements. However, both the manufacturer and the later study only provide a correction graph plotting the original against the corrected values without precise equations. The corrections are therefore made through visual interpretation (Fig. 2).

The corrections are calculated relatively to the horizontal impact. The two lower curves in the graph for negative impact angles −45° and −90° represent the situation when gravity "helps" the piston to rebound

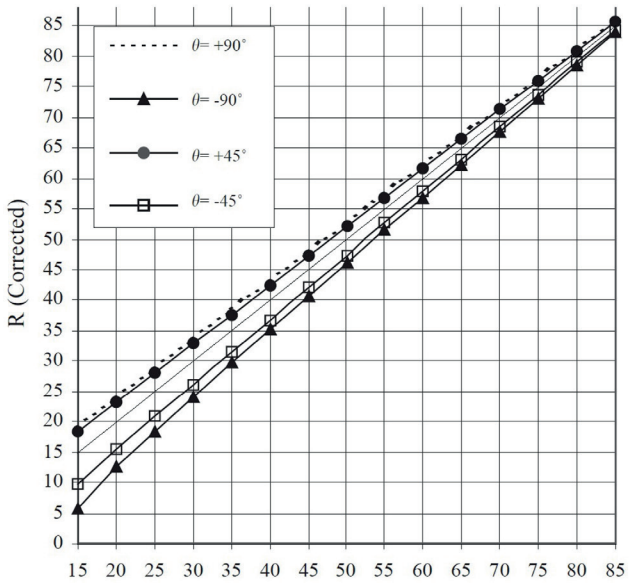

Fig. 2 Correction chart for inclination (Basu and Aydin 2004).

after the impact from below (overhanging surfaces). The recorded values are therefore higher than in the case of a horizontal impact and must be lowered back afterwards. The dependence of correction size on the original impact angle is obviously non-linear, which furthermore hinders the application of impact-angle corrections. In order to ensure homogeneous corrections for strictly integer R values, a set of thresholds was created for each recorded impact angle (Tab. 2).

3.3 Correction for aspect

The north-south orientation of the Belvedere Glacier valley controls the orographic wind direction. The combination of prevailing north or south winds predisposes higher weathering rates on the boulder sides facing the respective directions. The particular settings of most boulders did not allow for readings from all eight aspects, and often not even the basic four directions. Altogether, the boulder sides facing

Tab. 1 Characteristics of the sampled boulders; please note that the coloured categories of position are the same as in Fig. 1 and are retained in the following figures.

Boulder	Latitude (N)	Longitude (E)	Position	Rock type	Size (m)	Readings (n)
No. 1	45°56′49.76″	7°55′15.61″	on the surface	orthogneiss	10 × 15 × 15	50
No. 2	45°56′49.90″	7°55′14.30″	on the surface	orthogneiss	10 × 15 × 10	49
No. 3	45°56′48.21″	7°55′13.40″	moraine	orthogneiss	3 × 5 × 5	30
No. 4	45°56′59.36″	7°54′58.62″	on the surface	orthogneiss	15 × 25 × 30	38
No. 5	45°56′59.21″	7°55′00.00″	partly buried	orthogneiss	15 × 43 × 26	63
No. 6	45°57′03.68″	7°55′00.62″	on the surface	orthogneiss	13 × 16 × 10	40
No. 7	45°57′01.07″	7°55′05.74″	partly buried	orthogneiss	10 × 11 × 11	49
No. 8	45°57′06.61″	7°55′13.51″	on the surface	orthogneiss	2.5 × 4.5 × 4	41
No. 9	45°57′05.14″	7°55′04.45″	partly buried	orthogneiss	8 × 13 × 7	51
No. 10	45°57′06.84″	7°55′02.74″	partly buried	orthogneiss	12 × 10 × 8	50
No. 11	45°57′06.22″	7°55′02.23″	partly buried	orthogneiss	7 × 13 × 6	45
No. 12	45°57′12.74″	7°54′55.98″	moraine	orthogneiss	2 × 6 × 4	40
No. 13	45°57′15.34″	7°55′06.25″	on the surface	orthogneiss	12 × 18 × 12	42
No. 14	45°57′10.55″	7°55′07.25″	on the surface	orthogneiss	11 × 12 × 11	46
No. 15	45°57′29.76″	7°54′53.24″	moraine	paragneiss	4 × 6 × 4	41
No. 16	45°57′30.29″	7°54′53.93″	moraine	paragneiss	3 × 4 × 2.5	41
No. 17	45°57′32.36″	7°54′57.36″	moraine	paragneiss	6 × 3 × 3	47
No. 18	45°57′33.93″	7°54′59.67″	moraine	paragneiss	4 × 2 × 2	41
No. 19	45°57′49.20″	7°55′13.53″	supraglacial	paragneiss	6 × 3 × 1.5	40
No. 20	45°57′49.03″	7°55′11.92″	supraglacial	orthogneiss	4 × 4 × 2	41
No. 21	45°57′49.31″	7°54′51.68″	moraine	paragneiss	9 × 6 × 3	33
No. 22	45°57′50.26″	7°54′52.07″	moraine	paragneiss	10 × 8 × 6	31
No. 23	45°57′14.14″	7°55′03.08″	on the surface	orthogneiss	3 × 2 × 1	35
No. 24	45°57′11.48″	7°55′05.72″	partly buried	orthogneiss	2 × 1 × 2	30

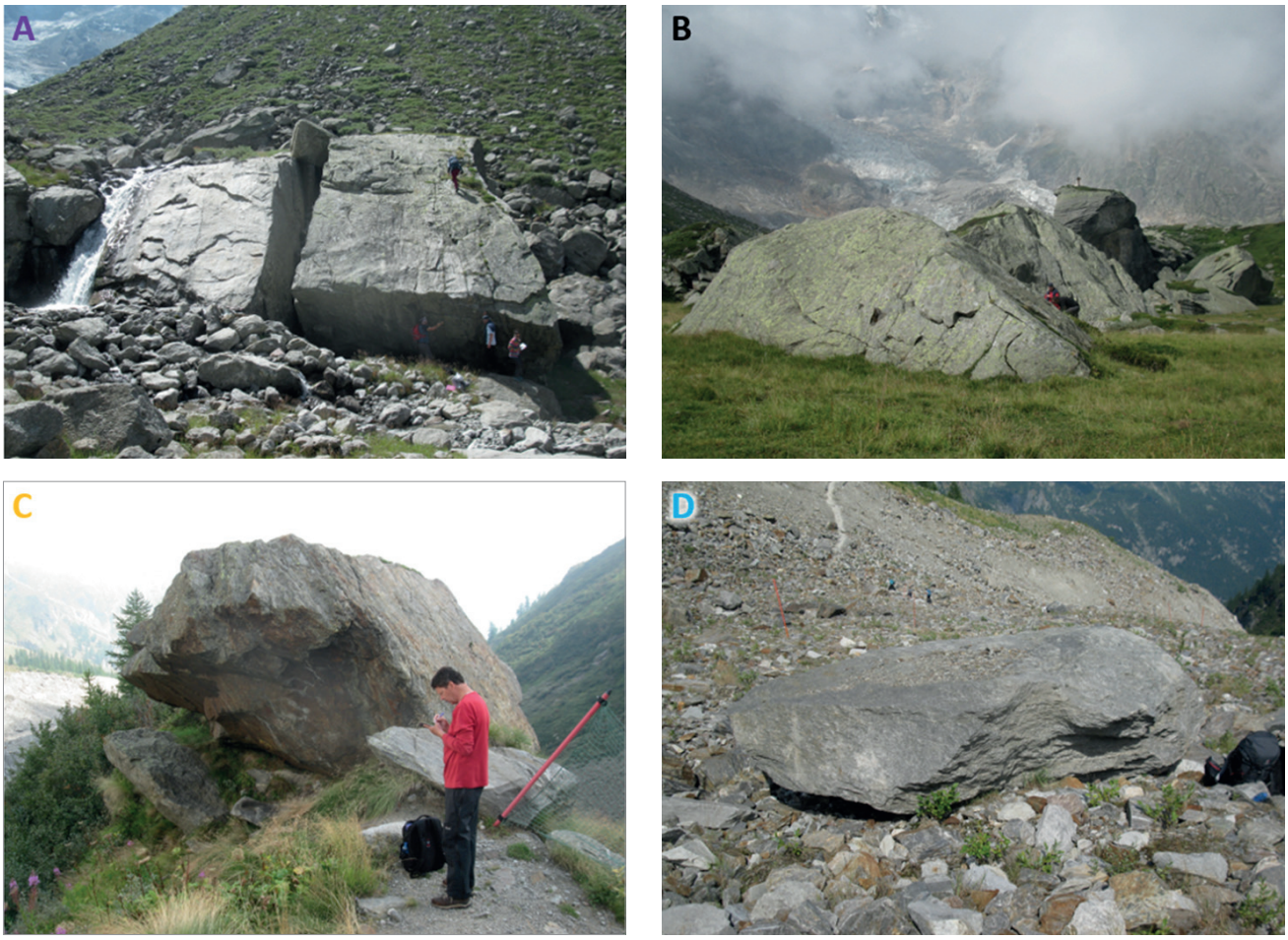

Fig. 3 Examples of boulders from all positional categories; A – boulder No. 2 located on surface; B – partly buried boulder No. 7; C – morainic boulder No. 17; D – supraglacial boulder No. 19.

the easterly directions were inspected most often. A combination of the above stated results in a potential aspect bias for most of the inspected boulders. To correct for the aspect, the deviation from the boulder average was calculated for each reading. Subsequently, the mean deviations for all eight aspects were obtained and these eight values served as the aspect corrections.

4. Results

Altogether, 1015 readings were collected from 24 boulders in two field campaigns (boulders No. 1–20 in 2022, and 21–24 in 2023). The number of readings per boulder ranged from 30 to 63, being randomly distributed among the accessible sides of each boulder. The boulders were split into four categories based on their location as seemed fit for the geomorphological interpretation. Fourteen boulders were located on the valley floor outside the moraine ridges, either partly buried within the plain or on its surface. Two blocks rested directly on the glacier surface (right lateral lobe), and eight were part of the lateral moraines of the Locce Glacier and the Belvedere Glacier (Fig. 1 and Fig. 3, Tab. 1). The two supraglacial and eight morainic boulders were presumed not to be rock avalanche-sourced and were included for comparison with the two first groups.

4.1 Uncorrected data

The average R values for each boulder calculated from the raw data are shown in Fig. 4A. The values span between 34 and 58, the vast majority of boulders fitting into the interval 40–55. The two boulders with extreme average R values were the only two located on the glacier surface. The second largest inhomogeneity of R values is among the morainic boulders (41–56.1), while the boulders positioned on the surface of the plain and those partly buried have considerably higher levels of homogeneity in R values (45.2–53.8 and 42.8–46.7, respectively).

The boulders partly buried within the plain tend to have lower R values than the boulders on the plain's surface. As lower R values mean a relatively older age, these data suggest two stages of boulder deposition. The obvious source of large boulders is the surrounding high rockwalls of the Monte Rosa massif. In prolonged periods of positive mass balance, the surface

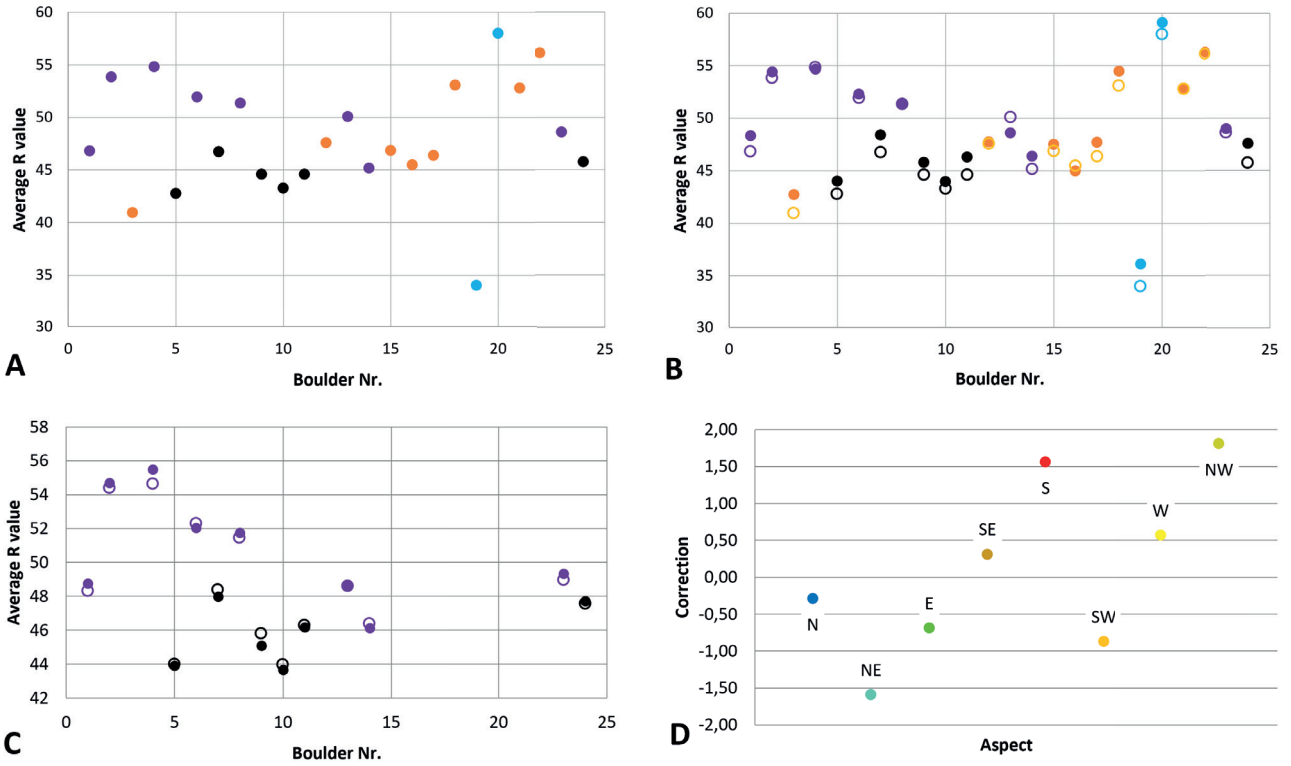

Fig. 4 Average R values of the sampled boulders; A – raw data; B – comparison of data before (hollow circles) and after the correction for inclination (filled circles); C – data before and after the correction for aspect (hollow and filled circles, respectively); D – calculated corrections for each aspect; colours in A–C correspond to the previous figures, colours in D correspond to Fig. 6.

of the Belvedere Glacier used to be well above current lateral moraine ridges. The rockfalls originating in the steep mountain faces could simply run over the glacier tongue and terminate between its right lateral moraine and the valley slopes.

4.2 Data corrected for inclination

The objective correction for the inclination of the boulder face created based on Basu and Aydin (2004) is presented in Tab. 2. The intervals for both the R values and impact angle are approximate; nonetheless, they are applied on the dataset. The raw data were divided into groups based on the inclination of the boulder face. For each group of inclinations (rows), the original R values define the correction that is found in the head of the respective column.

The correction for the surface inclination (Fig. 4B) slightly increased most of the average boulder R values (overall average change +1.1 per boulder) with only few exceptions (boulders No. 8, 14, and 16). The original scatter of values in the boulder positional categories, as well as the difference between partly buried boulders and those on the plain's surface were preserved. The generally positive compensation ensues from the absence of large overhanging surfaces that require negative compensations.

4.3 Data corrected for aspect

The very high scatter of R values in the morainic boulders and the two located directly on the glacier surface resulted in their exclusion from the final correction step, i.e., the compensation for the surface

Tab. 2 The inclination correction table; each cell gives the interval of R values corresponding to the respective combination of the impact angle and ensuing correction value.

Impact angle	Corrections					Impact angle	Corrections					
	4+	3+	2+	1+	0+		0–	1–	2–	3–	4–	5–
0–10°	32–	33–52	53+	x	x	**100°**	61+	60–	x	x	x	x
20–30°	x	29–44	45+	x	x	**110°**	x	40+	39–	x	x	x
40–50°	x	34–	35+	x	x	**120°**	x	65+	35–64	34–	x	x
55–60°	x	27–	28–54	55+	x	**135°**	x	x	55+	32–54	31–	x
70–75°	x	x	25–45	46+	x	**150°**	x	x	x	47+	33–46	32–
80°	x	x	x	54–	55+	**160°**	x	x	x	51+	36–50	35–

orientation. In addition, the prevailing wind directions may very well be obscured by the complex history of these boulders due to previous glacier transport and the unknown duration of their aspect to weathering. Therefore, only the boulders from the plain (on the surface and partly buried) were considered in the analysis of the orientation-related differences in R values. As there were only orthogneiss boulders in this subset, the aspect analysis should not be biased by lithology differences.

The most weathered boulder surfaces were oriented towards the south and northwest, whereas the most sheltered faces were oriented towards the northeast (resulting in positive and negative corrections, respectively, in Fig. 4D). However, there proved to be no distinct pattern, which would correspond to the north-south valley orientation.

Despite the uneven distribution of readings among the eight basic aspects, the corrections only slightly altered the average boulder R values (Fig. 4C). The calculated average change per boulder was negligible (+0.03).

5. Discussion

5.1 Geomorphological interpretation

Schmidt hammer readings from gneiss show higher dispersion due to the macroscopic properties of this rock type (Goudie 2006). The boulders of the Belvedere Glacier valley give average R values similar to the results listed by Goudie (2006) as the occasional impacts of crystals of stronger and weaker mineral disappeared in the most of the average data. The differentiation among the four boulder position categories showed to be very important. The boulders located directly on the glacier surface and on the lateral moraine ridges had a higher diversity in their average R values. This confirms their more complex history compared to the rock avalanche-sourced boulders of the surface of the plain due to the dynamicity of the supraglacial debris cover, and the activity of the proximal moraine sides. Both processes commonly allow for the appearance of rather fresh boulder surfaces with unknown previous evolution. Apparently, despite the neighbouring location of the boulders on the right glacier lobe (both No. 19 and 20), they must have experienced very different factors, one being strongly weathered and one still very fresh. The difference in lithology may be a contributing factor as well (No. 19 paragneiss whereas No. 20 orthogneiss). There were less differences among the boulders positioned on moraines, as the moraines were stable for tens of years before the onset of slope instabilities that unravelled the interior of the moraine ridges.

Higher homogeneity of average R values among the boulders positioned on the surface and partly buried as opposed to the supraglacial and morainic blocks supports a common origin of the two former groups. Rock avalanches from the surrounding high rockwalls represent the most probable source. Further differentiation between the boulders positioned on the surface of the plain (Fig. 5) and those partly buried (both groups consist strictly of orthogneiss boulders) should follow a simple rule. The boulders positioned on the surface should be younger and therefore give generally higher R values. This proved to be true for all boulders except one (No. 14, Fig. 4C), which would fit perfectly into the other positional category. Such misinterpretation is possible, as the only indication is the angle of the boulder sides at the surface. Even though its sides are apparently rounded at ground level, the central portion of boulder No. 14 may be protruding downwards into the plain.

The lithological disparity between orthogneiss and paragneiss are known to ensue in different weathering rates reflected in the R values (Longhi et al. 2024). This may be a contributing factor for the discrepancy between the two supraglacial boulders (No. 19 and No. 20) as suggested before. The same potential bias is inherent in most of the correction stages. However, the geomorphological interpretation regarding the

Fig. 5 The flat plain littered exclusively with orthogneiss boulders of varying deposition age (view towards the terminal moraine of the Locce Glacier where the Locce Lake is present); IDs of several block indicated.

source of the boulders of the plain was not affected as they were all orthogneiss boulders.

5.2 Significance of Corrections

The correction table (Tab. 2) created based on the findings by Basu and Aydin (2004) proved to be a suitable alternative to the classical graphical representation of the correction for the impact angle. As the majority of the readings were taken from surfaces inclined by about 90° and lower, the overall positive compensation was correctly in place. The correction may be viewed as redundant since it meant no significant change in the average R values, but this is not the case. It is unlikely for the boulders partly buried in the plain to have overhanging faces, as opposed to those positioned on the surface. Indeed, the corrected values for all the partly buried boulders were higher than the uncorrected values (meaning average inclination angles lower than 90°). However, some of the boulders on the surface (boulders No. 4 and 13) had a negative change due to the correction for the impact angle.

Similarly, the correction for the aspect did not bring significant changes. It seems that the uneven distribution of the accessible boulder faces among the basic directions was not uneven enough to cause a meaningful bias. The principle of similar representation of all aspects may not be as important as we thought, but then again, this is only one location with a specific orographic setting.

5.3 Aspect analysis

The south-north orographic setting of the upper portion of the Belvedere Glacier valley should ensue in the prevalence of northern and southern winds. This means that the boulder sides facing north and south should be more weathered as they experience higher changes in temperature and humidity. As the southern sides are shielded by the Monte Rosa massif, the most weathered boulder faces should be those oriented towards the north. On the other hand, the boulder sides facing west and east should be less weathered.

The highest positive compensation of boulder sides oriented towards the northwest and south (1.81 and 1.56, respectively) confirms this hypothesis. However, the lowest weathered sides facing north-east (negative compensation of −1.59) undermines it, as do the data from the western and eastern boulder sides. The faces oriented towards the west were significantly more weathered than the opposite sides, even though the compensations differ less (0.57 for the west and −0.69 for the east). In addition, the boulder sides facing north showed an average level of weathering (a compensation of only 0.31).

The data preclude even the back-up hypothesis of the level of weathering gradually decreasing from one aspect to the opposite one. Nevertheless, there still may be a logical explanation. The plain with the boulders is significantly closer to the eastern flank of the valley as the western half of the valley is occupied by the glacier tongue and both lateral moraines. The boulder sides facing east should therefore be more sheltered than the faces oriented towards the west. This is corroborated by less weathered northeastern and eastern boulder sides.

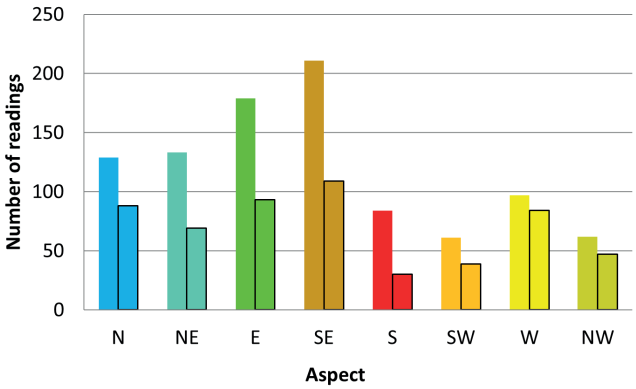

Fig. 6 Number of readings per aspect showing both all readings and those used for the aspect correction (unframed and framed columns, respectively).

The lowest number of readings suitable for the aspect analysis was obtained from the boulder sides facing south and southwest (both n < 40 in Fig. 6). Consequently, the average R values for each of these aspects were calculated based on the readings from three boulders. It is therefore possible that only more (or less) weathered faces may have been used. The resulting inaccuracy may be large. Nevertheless, this could not serve as an explanation to the conspicuous differences between the northwestern and northeastern aspects. Systematic misjudgement of aspects involving all the boulders may have been introduced as well. However, considering the high number of readings (each reading being an average of three values), such a systematic bias is not probable, and it should still leave the pattern of aspects intact, albeit distorted, and that is not the case.

6. Conclusions

The Schmidt hammer was applied to achieve the relative age dating of boulders in the Belvedere Glacier valley. A mixed set of 24 orthogneiss and paragneiss boulders of complex glacial and periglacial origin was sampled and split into four groups based on their location (boulders on the glacier, on the moraine, on the surface of the plain, and those partly buried within the plain). The raw data were corrected for the inclination angle and aspect. The results suggest an unpredictable history of the boulders located on the moraine and glacier surface. These exhibit large differences in

average R values between boulders of the same group. The majority of sampled blocks (58.3%) were located on the plain and their higher homogeneity of R values supports their common origin in rock avalanches from the surrounding rockwalls. The boulders partly buried within the plain are generally more weathered than those positioned on the surface (with comparable lithology) and are therefore older. There is only one exception in the case of boulder No. 14, which may have been misplaced in the wrong group (its base may be much lower in the centre than observed at the sides).

The corrections refined the data in a sense as the original overlap between the two groups of boulders of the plain was larger. No dramatic change in the results occurred but the sign of the correction usually varied boulder to boulder, so it proved to be relevant. For the first time, a table of objective inclination corrections was created based on Basu and Aydin (2004). It proved very useful as reading the correction from the scaling chart of limited size had been odious. The final analysis of aspect-related weathering differences showed no clear pattern. The most weathered seem to be boulder sides facing south and northwest, while the least weathered are the boulder faces oriented towards the northeast. The possible explanations include shielding by high relief and the potential bias introduced by the low number of boulders with sides of certain aspects (south and northwest).

The Schmidt hammer proved to be useful even in an environment with a complex geomorphological history and unsuitable rock types with macroscopic crystals. The precision of the results may probably increase with a larger set of sampled boulders. However, the Schmidt hammer technique is known to be sensitive to the moisture content of the rock surface. The high mountain environment offers only a limited period of dry conditions before the weather deteriorates. A potential next step may be a combination of a higher number of sampled boulders and several surfaces with known absolute dating, even though this may prove to be costly. The absolute dating would be especially useful for geomorphological mapping.

Acknowledgements

Both field campaigns were funded by the Project GAUK No. 258522 of the Charles University Grant Agency.
The Authors would like to thank the Province of Verbano-Cusio-Ossola for the permit of UAV and dendrogeomorphological surveys (dr. Andrea De Zordi, Settore III – Assetto del Territorio Georisorse e Tutela Faunistica, Servizio Rete Natura 2000 e Forestazione). The authors' gratitude belongs particularly to two anonymous reviewers and to the editors of AUC Geographica.

References

Aydin, A. (2015): ISRM Suggested Method for Determination of the Schmidt Hammer Rebound hardness: Revised Version. R. Ulusay (ed.) The ISRM Suggested Methods for Rock Characterization, Testing and Monitoring: 2007–2014. Springer, https://doi.org/10.1007/978-3-319-07713-0.

Basu, A., Aydin, A. (2004): A method for normalization of Schmidt hammer rebound values. International Journal of Rock Mechanics and Mining Sciences 41(7), 1211–1214, https://doi.org/10.1016/j.ijrmms.2004.05.001.

Betts, M. W., Latta, M. A. (2000): Rock surface hardness as an indication of exposure age: an archaeological application of the Schmidt hammer. Archeometry 42(1), 209–223, https://doi.org/10.1111/j.1475-4754.2000.tb00877.x.

Burda, J., Veselý, M., Řehoř, M., Vilímek, V. (2018): Reconstruction of a large runout landslide in the Krušné hory Mts. (Czech Republic). Landslides 15, 423–437, https://doi.org/10.1007/s10346-017-0881-0.

Day, M. J., Goudie, A. S. (1977): Field assessment of rock hardness using the Schmidt test hammer. British Geomorphological Research Group Technical Bulletin 18, 19–29.

Engel, Z., Traczyk, A., Braucher, R., Woronko, B., Křížek, M. (2011): Use of 10Be exposure ages and Schmidt hammer data for correlation of moraines in the Krkonoše Mountains, Poland/Czech Republic. Zeitschrift für Geomorphologie 55(2), 175–196, https://doi.org/10.1127/0372-8854/2011/0055-0036.

Fisher, L., Kääb, A., Huggel, C., Noetzli, J. (2006): Geology, glacier retreat and permafrost degradation as controlling factors of slope instabilities in high-mountain rock wall: the Monte Rosa east face. Natural Hazard Earth System Sciences 6(5), 761–772, https://doi.org/10.5194/nhess-6-761-2006.

Goudie, A. S. (2006): The Schmidt Hammer in geomorphological research. Progress in Physical Geography: Earth and Environment 30(6), 703–718, https://doi.org/10.1177/0309133306071954.

Haeberli, W., Epifani, F. (1986): Mapping the Distribution of Buried Glacier Ice – An Example from Lago Delle Locce, Monte Rosa, Italian Alps. Annals of Glaciology 8, 78–81, https://doi.org/10.3189/S026030550000118X.

Haryono, E., Day, M. (2004): Landform differentiation within the Gunung Kidul Kegelkarst, Java, Indonesia. Journal of Cave and Karst Studies 66(2), 62–69.

Kääb, A., Huggel., C., Barbero, S., Chiarle, M., Cordola, M., Epifani, F., Haeberli, W., Mortara, G., Semino, P., Tamburini, P., Viazzo, G. (2004): Glacier hazards at Belvedere Glacier and the Monte Rosa east face, Italian Alps: processes and mitigation. Internationales Symposion Interpraevent 2004 – Riva/Trient.

Karpuz, C., Paşamehmetoğlu, A. G. (1997): Field characterisation of weathered Ankara andesites. Engineering Geology 46(1), 1–17, https://doi.org/10.1016/S0013-7952(96)00002-6.

Klimeš, J., Vilímek, V., Omelka, M. (2009): Implications of geomorphological research for recent and prehistoric avalanches and related hazards at Huascaran, Peru. Natural Hazards 50, 193–209, https://doi.org/10.1007/s11069-008-9330-7.

Longhi, A., Guglielmin, M. (2020): Reconstruction of the glacial history after the Last Glacial Maximum in the Italian Central Alps using Schmidt's hammer R-values and crystallinity ratio indices of soils. Quaternary International 558, 19–27, https://doi.org/10.1016/j.quaint.2020.08.045.

Longhi, A., Morgan, D., Guglielmin, M. (2024): Reconstruction of rock avalanche history in Val Viola, (Upper Valtellina, Italian Central Alps) through ^{10}Be exposure ages, Schmidt Hammer *R* values, and surface roughness. Landslides 21, 949–962, https://doi.org/10.1007/s10346-024-02210-2.

Marr, P., Winkler, S., Dahl, S. O., Löffler, J. (2022): Age, origin and palaeoclimatic implications of peri- and paraglacial boulder-dominated landforms in Rondane, South Norway. Geomorphology 408: 108251, https://doi.org/10.1016/j.geomorph.2022.108251.

Matsukura, Y., Matsuoka, N. (1996): The effect of rock properties on rates of tafoni growth in coastal environments. Zeitschrift für Geomorphologie 106, 57–72, https://doi.org/10.1127/0372-8854/2007/0051S-0115.

Matthews, J. A., Shakesby, D. A. (1984): The status of the "Little Ice Age" in southern Norway: relative-age dating of Neoglacial moraines with Schmidt hammer and lichenometry. Boreas 13(3), 333–346, https://doi.org/10.1111/j.1502-3885.1984.tb01128.x.

Matthews, J. A., Winkler, S. (2022): Schmidt-hammer exposure-age dating – a review of principles and practice. Earth-Science Reviews 230, 104038, https://doi.org/10.1016/j.earscirev.2022.104038.

McEwen, L. J., Matthews, J. A., Owen, G. (2020): Development of a Holocene glacier-fed composite alluvial fan based on surface exposure-age dating techniques: the Illåe fan, Jotunheimen, Norway. Geomorphology 363: 107200, https://doi.org/10.1016/j.geomorph.2020.107200.

Nesje, A., Matthews, J. A., Linge, H., Bredal, M., Wilson, P., Winkler, S. (2021): New evidence for active talus-foot rock glaciers at Øyberget, southern Norway, and their development during the Holocene. The Holocene 31(11–12), 1786–1796, https://doi.org/10.1177/09596836211033226.

Pye, K., Goudie, A. S., Watson, A. (1986): Petrological influence on differential weathering and inselberg development in the Kora area of central Kenya. Earth Surface Processes and Landforms 11(1), 41–52, https://doi.org/10.1002/esp.3290110106.

Schmidt, E. (1950): Der Beton-Prüfhammer. Schweizerische Bauzeitung 68(28), 378–379.

Scotti, R., Brardinoni, F., Crosta, G. B., Cola, G., Mair, V. (2017): Time constraints for post-LGM landscape response to deglaciation in Val Viola, Central Italian Alps. Quaternary Science Reviews 177, 10–33, https://doi.org/10.1016/j.quascirev.2017.10.011.

Shakesby, R. A., Matthews, J. A., Owen, G. (2006): The Schmidt hammer as a relative-age dating tool and its potential for calibrated-age dating in Holocene glaciated environments. Quaternary Science Reviews 25, 2846–2867, https://doi.org/10.1016/j.quascirev.2006.07.011.

Sjöberg, R., Broadbent, N. (1991): Measurement and calibration of weathering, using the Schmidt Hammer, on wave washed moraines on the Upper Norrland coast, Sweden. Earth Surface Processes and Landforms 16(1), 57–64, https://doi.org/10.1002/esp.3290160107.

Stahl, T., Winkler, S., Quigley, M., Bebbington, M., Duffy, B., Duke, D. (2013): Schmidt hammer exposure-age dating (SHD) of late Quaternary fluvial terraces in New Zealand. Earth Surface Processes and Landforms 38(15), 1838–1850, https://doi.org/10.1002/esp.3427.

Tomkins, M. D., Dortch, J. M., Hughes, P. D. (2016): Schmidt hammer exposure dating (SHED), establishment and implications for the retreat of the last British Ice. Quaternary Geochronology 33, 46–60, https://doi.org/10.1016/j.quageo.2016.02.002.

Tomkins, M. D., Dortch, J. M., Hughes, P. D., Huck, J. J., Stimson, A. G., Delmas, M., Calvet, M., Pallàs, R. (2018): Rapid age assessment of glacial landforms in the Pyrenees using Schmidt hammer exposure dating (SHED). Quaternary Research 90(1), 26–37, https://doi.org/10.1017/qua.2018.12.

Waragai, T. (1999): Weathering processes on rock surfaces in the Hunza Valley, Karakoram, North Pakistan. Zeitschrift fur Geomorphologie, Supplementband 119, 119–136.

White, K., Bryant, R., Drake, N. (1998): Techniques for measuring rock weathering: application to a dated fan segment sequence in southern Tunisia. Earth Surface Processes and Landforms 23(11), 1031–1043, https://doi.org/10.1002/(SICI)1096-9837(1998110)23:11%3C1031::AID-ESP919%3E3.0.CO;2-G.

Yaalon, D. H., Singer, S. (1974): Vertical variation in trength and porosity of calcrete (Nari) chalk, Shefela, Israel and interpretation of its origin. Journal of Sedimentary Research 44, 1016–1023, https://doi.org/10.1306/212F6C17-2B24-11D7-8648000102C1865D.